Sub-dekahertz spectroscopy of $^{199}Hg^{+}$[†]

J.C. Bergquist*[a], R.J. Rafac[a], B.C. Young[b], J.A. Beall[a], W.M. Itano[a], and D.J. Wineland[a]
[a]National Institute of Standards and Technology, MS 847, 325 Broadway, Boulder, CO 80305
[b]Jet Propulsion Laboratory, MS 298-100, 4800 Oak Grove Drive, Pasadena, CA 91109

ABSTRACT

Using a laser that is frequency-locked to a Fabry-Pérot etalon of high finesse and stability, we probed the $5d^{10}6s\ ^2S_{1/2}$ ($F = 0$, $m_F = 0$) ↔ $5d^9 6s^2\ ^2D_{5/2}$ ($F = 2$, $m_F = 0$) electric-quadrupole transition of a single laser-cooled $^{199}Hg^+$ ion stored in a cryogenic radio-frequency ion trap. We observed Fourier-transform limited linewidths as narrow as 6.7 Hz at 282 nm (1.06 x 10^{15} Hz). The functional form and estimated values of some of the frequency shifts of the $^2S_{1/2} \leftrightarrow {}^2D_{5/2}$ "clock" transition (including the quadrupole shift), which have been calculated using a combination of measured atomic parameters and *ab initio* calculations, are given.

Keywords: Lasers, atomic spectroscopy, cooling and trapping, atomic frequency standards, optical clocks.

1. Introduction

For spectroscopy and clocks, fluctuations in frequency measurement are expressed fractionally as $\sigma_y(\tau) = \Delta\nu_{meas}(\tau)/\nu_0$, where τ is the total measurement time. When the measured stability is limited by quantum fluctuations in state detection, $\sigma_y(\tau) = C(2\pi\nu_0)^{-1}(N\,\tau_{probe}\,\tau)^{-1/2}$, where C is a constant of order unity, N is the number of atoms, and τ_{probe} is the interrogation time. For atomic clocks, the highest accuracies and the greatest stabilities have been achieved by locking a microwave oscillator to a hyperfine transition in the electronic ground state (see, for example, the contribution by A. Clairon in these Proceedings). Since the fractional frequency instability $\sigma_y(\tau)$ of a frequency and time standard is inversely proportional to its frequency, a promising route to realizing clocks with stability significantly higher than present-day standards is to use optical frequencies. However, there are significant obstacles that so far have thwarted the development of an optical clock. Principal among these are the requirements of a spectrally pure and stable laser, a narrow reference transition that can be probed with a high signal-to-noise (S/N) ratio, and a device fast enough to count optical frequencies. If high accuracy is also desired, then either perturbations to the reference transition must be small or the uncertainty in measuring the frequency shifts of the reference transition in the perturbed system must be small.

Recently, the major technical barriers to the development of an optical clock were eliminated. Two years ago, lasers suitable for probing sub-hertz atomic linewidths were demonstrated,[1,2] and in the past year, precision, optical-frequency measuring devices based on mode-locked femtosecond lasers have emerged.[3,4,5] It has long been recognized that a frequency and time standard based on an optical transition in a single ion that is tightly confined in a benign environment and virtually at rest could be made both highly stable *and accurate*.[6] In this paper, we summarize the measurement of the $5d^{10}6s\ ^2S_{1/2}$ ($F = 0$, $m_F = 0$) ↔ $5d^9 6s^2\ ^2D_{5/2}$ ($F = 2$, $m_F = 0$) electric-quadrupole-allowed transition ($\lambda \approx 282$ nm) in a single, laser-cooled $^{199}Hg^+$ ion for which a linewidth $\Delta\nu \approx 6.7$ Hz is observed.[7] The frequency of a laser can be locked to this transition to provide an extremely stable and reproducible frequency reference. Elsewhere[8] (and in these Proceedings: see S.A. Diddams *et al.,* "A compact femtosecond-laser-based optical clockwork") we report an absolute measurement of the frequency ν_0 of this $^2S_{1/2} \leftrightarrow {}^2D_{5/2}$ "clock" transition, $\nu_0 = 1\,064\,721\,609\,899\,143(10)$ Hz, which represents the most precise measurement of an optical frequency ever made. We also report recent calculations[9] of perturbations to the ($F = 0$, $m_F = 0$) to ($F = 2$, $m_F = 0$) hyperfine component of the $^2S_{1/2} \leftrightarrow {}^2D_{5/2}$ transition that include the quadratic Zeeman shift, the scalar and tensor quadratic Stark shifts, and the interaction between an external static electric field gradient and the atomic quadrupole moment. The quadrupole shift is likely to be the most difficult to evaluate in such a frequency standard and may have a magnitude as large as 1 Hz for a single ion in a spherical rf quadrupole trap.

*email: berky@boulder.nist.gov

2. Spectroscopy of $^{199}Hg^{+}$

2.1 The atomic system, probe laser, and trap

A partial energy-level diagram of $^{199}Hg^{+}$ is shown in Fig. 1. The 282 nm radiation used to drive the S-D clock transition is produced in a nonlinear crystal as the second harmonic of a dye laser oscillating at 563 nm. The frequency of the dye-laser's radiation is made to match the resonance of a single longitudinal mode of a high-finesse Fabry-Pérot cavity that is temperature-controlled and supported on an isolation platform.[1,2] The frequency-stabilized laser light is sent through a single-mode optical fiber to the table holding the ion trap. Mechanical and acoustical vibrations of the fiber broaden the laser spectrum by about 1 kHz. The phase and frequency noise caused by the journey through the fiber is sensed and removed using a method[2] that is similar to that described in references 10 and 11. Finally, the frequency of the 563 nm light is shifted away from the cavity resonance and on to the ion resonance by passing the 563 nm radiation through an acousto-optic crystal and then doubling the frequency of the shifted light by harmonic generation in a deuterated ammonium-dihydrogen-phosphate crystal.

Two types of cryogenic ion traps have been used in our most recent measurements; a linear quadrupole trap[7] and a spherical Paul trap.[8] For both systems, a single mercury ion is loaded into the trap by ionizing a mercury atom from a thermal source with a pulsed electron beam. Under typical operating conditions, the radial secular frequency of the trapped ion varies between 1.2 and 1.5 MHz. Biasing electrodes are mounted outside the trap electrodes to cancel any stray static electric fields that may be present. Since the electrodes in both traps are gold coated and can be heated, oxidation is precluded and any charging of the electrodes is minimized.

The ion is laser-cooled to near the 1.7 mK Doppler limit by driving the $5d^{10}6s\ ^2S_{1/2}$ ($F = 1$) $\leftrightarrow$ $5d^{10}6p\ ^2P_{1/2}$ ($F = 0$) cycling transition at 194 nm (Fig. 1). Because of weak off-resonant pumping into the $^2S_{1/2}$ ($F = 0$) state, we employ a second 194 nm source, phase-locked to the first with a 47 GHz offset, that returns the ion to the ground state $F = 1$ hyperfine level. We tolerate the complication of a re-pumper, since only isotopes with nonzero nuclear spin can have transitions that are first-order insensitive to magnetic field fluctuations. This provides immunity from fluctuations of the ambient field and significantly relaxes the requirements for control and shielding of the magnetic environment. Previous experiments using mercury were performed at room temperature and at a pressure of approximately 10^{-7} Pa.[10] Under those conditions, the background gas pressure was large enough that when the ion was irradiated with the 194 nm light, it would be lost due to chemical reaction after a few minutes. Partly as a means to help reduce this loss, the ion trap is now housed in a vacuum system held at liquid-helium temperature. Single ion hold times have now exceeded 100 days, and any loss of an ion has been caused either by a deliberate or accidental action of the operator. Vibrations of the supported trap structure relative to the optical table are sensed and removed with an additional stage of Doppler cancellation, where the correction signal is derived from optical heterodyne detection of a motion-sensing beam reflected from a mirror that is rigidly fixed to the trap support structure.[7,10] The cancellation is not ideal, because the sensing beam is steered by additional optical elements and its path deviates slightly from overlap with the probe beam near the trap. Measurements indicate that this optical path difference can contribute as much as 2 Hz to the spectral width of the 282 nm probe laser in the reference frame of the ion.

We monitor the ion and deduce its electronic state using light scattered from the cooling transition. Fluorescence at 194 nm is collected by a five-element *f*/1 objective located inside the cryostat. The scattered light is imaged outside the dewar, spatially filtered, and then relayed with a second lens to either an imaging tube or to a side-on photomultiplier tube. Transitions to the D state are detected using the technique of "electron shelving," which infers the presence of the atom in the metastable level through the absence of scattering from the strong laser-cooling transition.[6,12,13] Radiation from the 194 and 282 nm sources is admitted to the trap sequentially to prevent broadening of the quadrupole transition by the cooling radiation. Typical count rates using the more efficient photomultiplier tube are 12 000 Hz for a single ion when the frequency of the 194 nm source is detuned below resonance with the cooling transition by about ½ the natural linewidth. The background rate is only about 25 Hz when the ion is shelved in the metastable level. Hence, each clock transition to the D level can be detected in only a few milliseconds with near unit efficiency.

Spectra of the recoilless component of the $^2S_{1/2}$ ($F = 0$, $m_F = 0$) $\leftrightarrow$ $^2D_{5/2}$ ($F = 2$, $m_F = 0$) clock transition were obtained for a range of probe times and laser intensities by laser cooling for a short period, preparing the ion in the $F = 0$ ground state by blocking the repumping laser, and then interrogating the quadrupole transition. The spectra are built up from multiple bi-directional scans of the 282 nm probe-laser frequency. Since the frequency of the probe laser can drift, we incorporate a locking step in between pairs of positive- and negative-going frequency sweeps through the quadrupole resonance. During the locking sequence, we step the frequency of the probe laser alternately to the maximum slope on either side of the S-D

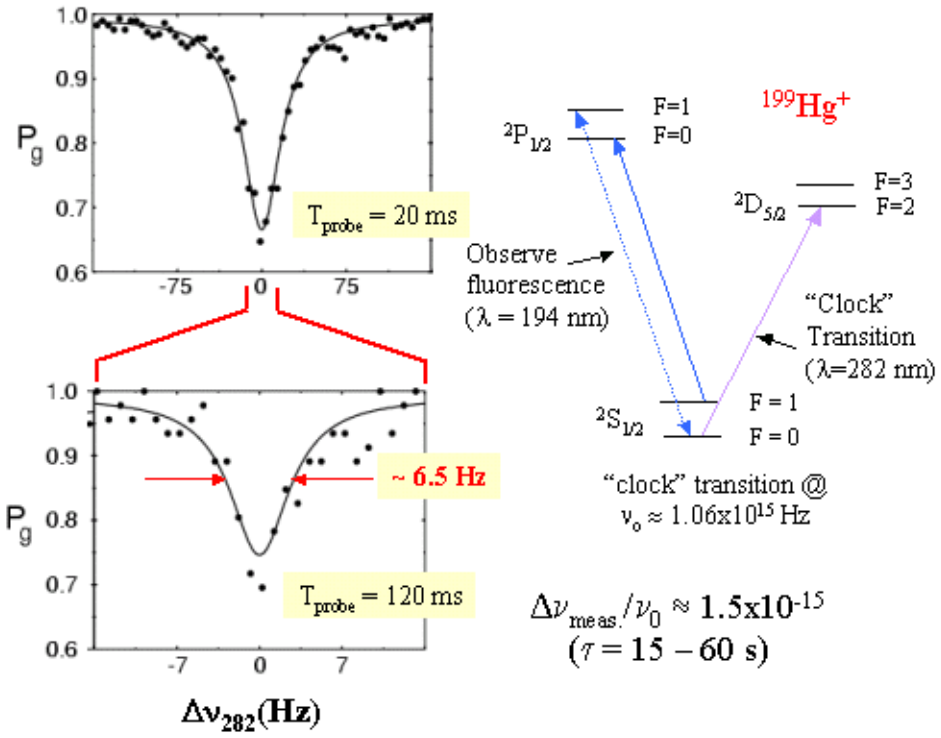

Figure 1: The simplified optical level diagram of $^{199}Hg^+$is depicted on the right. Quantum-jump absorption spectra of the $^2S_{1/2}$ ($F = 0$, $m_F = 0$) ↔ $^2D_{5/2}$ ($F = 2$, $m_F = 0$) clock transition for two different probe times are shown on the left. $\Delta\nu_{282}$ is the frequency detuning of the 282 nm probe laser, and P_g is the probability of finding the atom in the ground state after the probe radiation is applied. In the top spectrum (averaged over 292 sweeps), the probe-pulse period was 20 ms; in the bottom spectrum (averaged over 46 sweeps), the probe period was 120 ms. The observed linewidths are consistent with the Fourier-transform limit of the probe period at 40(2) Hz and 6(1) Hz respectively.

quadrupole resonance, probe for a fixed time τ_{servo}, and then look for transitions to the D level. Typically, we make 48 measurements on each side of the resonance during each lock cycle before steering the mean frequency of the 282 nm radiation to line center. Our servo is a simple integrator that works to minimize the asymmetry between the number of detected transitions on the high- and low-frequency sides of the resonance. In this fashion, variations in the frequency of the 282 nm laser for times exceeding several seconds are reduced.

Two examples of the spectra are plotted in Fig. 1. The probe time for the lower resolution spectrum is 20 ms and the probe time for the higher resolution signal is 120 ms. In both cases, the linewidths are transform limited by the finite probe time at 40(2) Hz and 6(1) Hz, respectively. The carrier transition amplitude is a function of the vibrational quantum number n.[14] For the spectra shown in Fig. 1, the trapping parameters gave $\langle n \rangle \approx 35$ at the Doppler cooling limit ($\langle n \rangle \approx 20$ for the spherical trap at the Doppler cooling limit). Hence, it is not possible to transfer the electron to the D level with unit probability. The observed signals are in good agreement with the theoretical expectation, and the signal loss for $\tau_{probe} = 120$ ms is consistent with applying the probe time for a period that exceeds the natural lifetime of the $^2D_{5/2}$ state by 33 %. In future experiments, we plan to reduce $\langle n \rangle$ to less than 1 toward improving the signal amplitude and S/N ratio.

3. External field shifts to the quadrupole transition

While the $^2S_{1/2}$ ($F = 0$, $m_F = 0$) ↔ $^2D_{5/2}$ ($F = 2$, $m_F = 0$) hyperfine component has no linear Zeeman shift, it does have a quadratic Zeeman shift. In addition, there is a second-order Stark shift and a shift due to the interaction between a static electric-field gradient and the D-state atomic electric-quadrupole moment. None of these shifts has yet been measured accurately but their values have recently been calculated by one of us.[9] While these values may be imprecise, it is useful to know the functional form of the perturbation. For example, the quadrupole shift can be eliminated by averaging the S-D

transition frequency over three mutually orthogonal magnetic-field orientations, independent of the orientation of the electric-field gradient, and is zero in lowest order for the $^2S_{1/2}$ ($F = 2$, $m_F = 0$) ↔ $^2D_{3/2}$ ($F = 0$, $m_F = 0$) hyperfine component in $^{201}Hg^+$.

The quadratic Zeeman shift can be calculated if the hyperfine constants and electronic and nuclear g-factors are known. Similarly, the quadratic Stark shift can be calculated from a knowledge of the electric-dipole oscillator strengths. The quadrupole shift depends on the atomic wavefunctions. Some of these parameters have been measured, such as the hyperfine constants and some of the oscillator strengths. In Ref. 9, values for parameters for which there are neither measured values nor published calculations are estimated using the Cowan atomic-structure codes.[15] The Cowan codes are based on the Hartree-Fock approximation with some relativistic corrections. The odd-parity configurations used in these calculations were $5d^{10}np$ (n = 6,7,8,9), $5d^{10}5f$, $5d^96s6p$, $5d^96s7p$, $5d^96s5f$, and $5d^86s^26p$. The even-parity configurations were $5d^{10}ns$ (n = 6,7,8,9,10), $5d^{10}nd$ (n = 6,7,8,9), $5d^96s^2$, $5d^96s7s$, $5d^96s6d$, and $5d^96p^2$. Recently, Sansonnetti and Reader have made new measurements of the spectrum of Hg^+ and classified many new lines.[16] They also carried out a least-squares adjustment of the energy parameters in order to match the observed energy levels. Those adjusted parameters were used for the calculations in Ref. 9.

3.1 Quadratic Zeeman shift

In order to calculate the energy shifts due to the hyperfine interaction and to an external magnetic field $\boldsymbol{B} \equiv B\,\hat{\mathbf{z}}$, we define effective Hamiltonian operators H_S and H_D that operate within the subspaces of hyperfine levels associated with the electronic levels $5d^{10}6s\ ^2S_{1/2}$ and $5d^96s^2\ ^2D_{5/2}$ respectively:

$$H_S = hA_S\boldsymbol{I}\cdot\boldsymbol{J} + g_J(S)\mu_B\boldsymbol{J}\cdot\boldsymbol{B} + g'_I\mu_B\boldsymbol{I}\cdot\boldsymbol{B}$$

$$H_D = hA_D\boldsymbol{I}\cdot\boldsymbol{J} + g_J(D)\mu_B\boldsymbol{J}\cdot\boldsymbol{B} + g'_I\mu_B\boldsymbol{I}\cdot\boldsymbol{B},$$

where A_S and A_D are the dipole hyperfine constants, $g_J(S)$ and $g_J(D)$ are the electronic g-factors, g'_I is the nuclear g-factor, h is the Planck constant, and μ_B is the Bohr magneton. All of the parameters entering H_S and H_D are known from experiments, although a more accurate measurement of the excited-state electronic g-factor would improve our estimate of the quadratic Zeeman shift of the $^2D_{5/2}$ level. So far, the best determination of $g_J(D)$ (= 1.1980(7)) is derived from a conventional grating spectroscopic measurement of the $5d^{10}6p\ ^2P_{3/2}$ to $5d^96s^2\ ^2D_{5/2}$ at 398 nm in $^{198}Hg^+$.[17] The difference in $g_J(S)$ or $g_J(D)$ between $^{198}Hg^+$ and $^{199}Hg^+$ is estimated to be much less than the experimental uncertainties. The determination of $g_J(D)$ could be improved by measuring the optical frequency difference between two components of the 282 nm line and the frequency of a ground-state hyperfine transition at the same magnetic field. Since the uncertainty in the quadratic Zeeman shift is due mainly to the uncertainty in $g_J(D)$, it is useful to improve the experimental value and/or make an accurate theoretical estimate. The Cowan-code calculation gives a theoretical value of $g_J(D)$ of 1.19985,[9] which disagrees with the present experimental value by about 2.6 times the stated measurement uncertainty. From a similar comparison of the calculated value of $g_J(D)$ for neutral gold (which is isoelectronic to Hg^+) to its accurately measured experimental value, we might expect that the error in the calculated value of $g_J(D)$ of $^{199}Hg^+$ to be less than 1×10^{-4}. However, uncalculated terms may decrease the theoretical precision.

For low magnetic fields (< 1 mT), it is sufficient to calculate the energies of the Zeeman sub-levels of the $^2S_{1/2}$ ground electronic level and those of the $^2D_{5/2}$ electronic level to second order in B. For a magnetic field value of 0.1 mT, the quadratic shift of the $^2S_{1/2}$ ($F = 0$, $m_F = 0$) ↔ $^2D_{5/2}$ ($F = 2$, $m_F = 0$) clock transition is –189.25(28) Hz, where the uncertainty is dominated by the uncertainty in the experimental value of $g_J(D)$. If instead we use the calculated value of $g_J(D)$, the quadratic shift for B = 0.1 mT is –189.98 Hz, where the uncertainty may be less than 0.02 Hz but is difficult to estimate.[9]

3.2 Quadratic Stark shift

The theory of the quadratic Stark shift in free atoms has been described thoroughly by Angel and Sandars.[18] The Stark Hamiltonian is

$$H_E = -\boldsymbol{\mu}\cdot\boldsymbol{E},$$

where $\boldsymbol{\mu}$ is the electric-dipole moment operator,

$$\boldsymbol{\mu} = -e\sum\boldsymbol{r}_i,$$

and $\boldsymbol{E}$ is the applied external electric field. In the latter expression, $\boldsymbol{r}_i$ is the position operator of the ith electron, measured relative to the nucleus, and the summation is over all electrons. For an atom with zero nuclear spin, and to second order in the electric field, the Stark shift of the set of sublevels $|\gamma JM_J\rangle$ depend on two parameters, $\alpha_{\text{scalar}}(\gamma, J)$ and $\alpha_{\text{tensor}}(\gamma, J)$, called the scalar and tensor polarizabilities. Here, γ designates the electronic level, J the electronic angular momentum, and M_J is the eigenvalue of J_z. In principle, when both magnetic and electric fields are present but not parallel, the energy shifts of the levels are obtained by simultaneously diagonalizing the hyperfine, Zeeman, and Stark Hamiltonians. In practice, the Zeeman shifts normally dominate the Stark shifts, so H_E does not affect the diagonalization. We also note that the tensor polarizability is zero for levels with $J < 1$, such as the ground electronic level in Hg^+. For an atom with nonzero nuclear spin I, we make the approximation that the hyperfine interaction does not modify the electronic part of the atomic wavefunctions . This approximation is adequate for the evaluation of the Stark shift of the S-D optical clock transition in $^{199}Hg^+$.

In Ref. 9, the polarizabilities for the Hg^+ $5d^{10}6s\ ^2S_{1/2}$ and $5d^96s^2\ ^2D_{5/2}$ levels were evaluated. The tensor polarizability is much smaller than the scalar polarizabilities and, in any case, contributes nothing if the external field, such as the blackbody radiation field, is isotropic. The net shift of the optical clock transition due to the scalar polarizabilities is $\frac{1}{2}[\alpha_{\text{scalar}}(S,1/2) - \alpha_{\text{tensor}}(D,5/2)]E^2$. In frequency units, the shift is $-1.14 \times 10^{-3}\ E^2$ Hz, where E is expressed in V/cm. The error in the coefficient is difficult to estimate, particularly since it is a difference of two quantities of nearly equal magnitude. However, the total shift of either state is small for typical experimental conditions. If the electric field is time dependent, as for the blackbody field, the mean square value of the field is taken. At a temperature of 300 K, the shift of the S-D clock transition due to the blackbody field is –0.079 Hz. Since the blackbody electric field is proportional to the fourth power of the temperature, in our cryogenic environment the Stark shift due to blackbody radiation is negligible. Finally, for a single, laser-cooled ion in a Paul trap, the mean square trapping fields at the site of the ion can be made small enough that the Stark shifts are not likely to be observable.[19]

3.3 Electric quadrupole shift

The atomic quadrupole moment arises from the departure of the electronic charge distribution of an atom from spherical symmetry. The interaction of the atomic quadrupole moment with external field gradients, such as those that might be generated by the electrodes of an ion trap, is analogous to the interaction of a nuclear quadrupole moment with the electric field gradients due to the atomic electrons. The Hamiltonian describing the interaction of external electric-field gradients with the atomic quadrupole moment is

$$H_Q = \boldsymbol{E}^{(2)} \cdot \boldsymbol{\Theta}^{(2)},$$

where $\boldsymbol{E}^{(2)}$ is a tensor describing the gradients of the external electric field at the position of the ion, and $\boldsymbol{\Theta}^{(2)}$ is the electric-quadrupole operator for the atom. As long as the energy shifts due to H_Q are small relative to the Zeeman shifts, which is usually the case in practice, H_Q can be treated as a perturbation. In that case, it is necessary only to evaluate the matrix elements of H_Q that are diagonal in the basis states $|\gamma JFM_F\rangle$, where $\boldsymbol{F}$ is the total atomic angular momentum, including the nuclear spin $\boldsymbol{I}$, and M_F is the eigenvalue of F_z with respect to the laboratory frame, where the magnetic field is oriented along the z axis. The diagonal matrix elements of H_Q in the laboratory frame are[9]

$$\langle \gamma JFM_F | H_Q | \gamma JFM_F \rangle =$$

$$\frac{-2[3M_F^2 - F(F+1)]A(\gamma JF\|\Theta^{(2)}\|\gamma JF)}{[(2F+3)(2F+2)(2F+1)2F(2F-1)]^{1/2}}[(3\cos^2\beta - 1) - \varepsilon \sin^2\beta(\cos^2\alpha - \sin^2\alpha)]. \qquad (1)$$

It is relatively straightforward to show, by directly integrating the angular factor in square brackets in the above equation, that the average value of the diagonal matrix elements of H_Q, taken over all possible orientations of the laboratory frame with respect to the principal-axis frame,[20] is zero. It is less obvious, but nevertheless true, that the average taken over *any* three mutually perpendicular orientations of the laboratory z quantization axis is also zero.[9] This provides a method for eliminating the quadrupole shift from the observed transition frequency. The magnetic field, with constant magnitude, must be oriented in three mutually orthogonal directions; the average of the clock transition frequencies taken under these three conditions does not contain the quadrupole shift.

The reduced matrix element in Eq.(1) is, in the IJ-coupling approximation,

$$(\gamma(IJ)F\left\|\Theta^{(2)}\right\|\gamma(IJ)F) = (-1)^{I+J+F}(2F+1)\begin{Bmatrix} J & 2 & J \\ F & I & F \end{Bmatrix}\begin{pmatrix} J & 2 & J \\ -J & 0 & J \end{pmatrix}^{-1}\Theta(\gamma, J),$$

where I is included in the state notation in order to specify the order of coupling of I and J. For the particular case of the $^{199}Hg^{+}$ $5d^{9}6s^{2}\,{}^{2}D_{5/2}$ level, the reduced matrix elements are

$$(D\,5/2\,2\left\|\Theta^{(2)}\right\|D\,5/2\,2) = 2\sqrt{\frac{14}{5}}\Theta(D,5/2),$$

$$(D\,5/2\,3\left\|\Theta^{(2)}\right\|D\,5/2\,3) = 2\sqrt{\frac{21}{5}}\Theta(D,5/2).$$

Since the Cowan-code calculation shows that there is very little mixing in the $^{199}Hg^{+}$ $5d^{9}6s^{2}\,{}^{2}D_{5/2}$ level, Θ(D,5/2) can be reduced to a matrix element involving only the $5d$ orbital:[9]

$$\Theta(D,5/2) = \frac{e}{2} < 5d^{2}d_{5/2}, m_j = 5/2\left|3z^{2}-r^{2}\right|5d^{2}d_{5/2}, m_j = 5/2 >,$$

$$= -\frac{2e}{7} < 5d\left|r^{2}\right|5d >.$$

In this case, the matrix element is negative because the quadrupole moment is due to a single *hole* in the otherwise filled $5d$ shell rather than to a single electron. Again, according to the Cowan-code calculation,

$$< 5d\left|r^{2}\right|5d >= 2.324\,a_0^{2} = 6.509\times10^{-17}\ \mathrm{cm}^{2},$$

where a_0 is the Bohr radius. Since the quadrupole shifts are zero in the $5d^{10}6s\,{}^{2}S_{5/2}$ level, the quadrupole shift of the $^{199}Hg^{+}$ optical clock transition is due entirely to the shift of the |D 5/2 2 0> state, and is given by

$$\begin{aligned} < \mathrm{D}\,5/2\,2\,0\left|H_{\mathrm{Q}}\right|\mathrm{D}\,5/2\,2\,0 >&= \frac{4}{5}A\Theta(\mathrm{D},5/2)[(3\cos^{2}\beta-1)-\varepsilon\sin^{2}\beta(\cos^{2}\alpha-\sin^{2}\alpha)],\\ &= -\frac{8}{35}Ae < 5d\left|r^{2}\right|5d > [(3\cos^{2}\beta-1)-\varepsilon\sin^{2}\beta(\cos^{2}\alpha-\sin^{2}\alpha)],\\ &\approx -3.6\times10^{-3}\,hA[(3\cos^{2}\beta-1)-\varepsilon\sin^{2}\beta(\cos^{2}\alpha-\sin^{2}\alpha)]\ \mathrm{Hz}, \end{aligned}$$

where A is expressed in units of V/cm^2. Thus, for typical values $A \approx 10^3$ V/cm^2 and $|\varepsilon| \le 1$, the quadrupole shift is on the order of 1 Hz.[9] We also note that states with zero total angular momentum have no quadrupole shift. Thus, the $^{2}S_{1/2}$ ($F = 2$, $m_F = 0$) $\leftrightarrow$ $^{2}D_{3/2}$ ($F = 0$, $m_F = 0$) hyperfine component in $^{201}Hg^{+}$, for which the nuclear spin I is 3/2, has no quadrupole shift. Similar strategies to eliminate the quadrupole shift could be used on other potential optical-clock ions such as Ca^{+}, Sr^{+}, Ba^{+}, and Yb^{+}.

ACKNOWLEDGMENTS

We acknowledge the support of the Office of Naval Research. This work was also supported through a Cooperative Research and Development Agreement with Timing Solutions, Corp., Boulder, Colorado. We thank Dr. C.J. Sansonetti for making available his results (Ref. 16) prior to their publication. We would also like to thank R. Drullinger, M. Lombardi, and D. Smith for their careful reading of this manuscript.

REFERENCES

[†] Work of U.S. government. Not subject to U.S. copyright.

1. B.C. Young, F.C. Cruz, W.M. Itano, and J.C. Bergquist, "Visible lasers with subhertz linewidths," *Phys. Rev. Lett.* **82**, pp. 3799-3802, 1999.

2. B.C. Young, R.J. Rafac, J.A. Beall, F.C. Cruz, W.M. Itano, D.J. Wineland, and J.C. Bergquist, "Hg^+ optical frequency standard: recent progress," in *Laser Spectroscopy XIV International Conference*, ed. by R. Blatt, J. Eschner, D. Leibfried, and F. Schmidt-Kaler (World Scientific, Singapore, 1999) pp. 61-70.

3. Th. Udem, J. Reichert, R. Holzwarth, and T.W. Hänsch, "Absolute optical frequency measurement of the cesium D_1 line with a mode-locked laser," *Phys. Rev. Lett.***82**, pp. 3568-3571, 1999.

4. D.J. Jones, S.A. Diddams, J.K. Ranka, A. Stentz, R.S. Windeler, J.L. Hall, and S.T. Cundiff, "Carrier-envelope phase control of femtosecond mode-locked lasers and direct optical frequency synthesis, " *Science* **288**, pp. 635-639, 2000.

5. S.A. Diddams, D.J. Jones, J. Ye, S.T. Cundiff, J.L. Hall, J.K. Ranka, R.S. Windeler, R. Holzwarth, Th. Udem, and T. W. Hänsch, "Direct link between microwave and optical frequencies with a 300 THz femtosecond laser comb," *Phys. Rev. Lett.* **84**, pp. 5102-5105, 2000.

6. H.G. Dehmelt, "Coherent spectroscopy on single atomic system at rest in free space II," *J. Phys. (Paris) Colloq.* **42**, pp. C8-299 to C8-305, 1981.

7. R.J. Rafac, B.C. Young, J.A. Beall, W.M. Itano, D.J. Wineland, and J.C. Bergquist, "Sub-dekahertz ultraviolet spectroscopy of $^{199}Hg^+$," *Phys. Rev. Lett.* **85**, pp. 2462-2465, 2000.

8. Th. Udem, S.A. Diddams, K.R. Vogel, C.W. Oates, E.A. Curtis, W.D. Lee, W.M. Itano, R.E. Drullinger, J.C. Bergquist, and L. Hollberg, "Absolute Frequency Measurements of the Hg^+ and Ca optical clock transitions with a femtosecond laser," submitted to *Phys. Rev. Lett*.

9. W.M. Itano, "External-field shifts of the $^{199}Hg^+$ optical frequency standard," *J. Res. NIST*, in press, 2001.

10. J.C. Bergquist, W.M. Itano, and D.J. Wineland, "Laser stabilization to a single ion," in *Frontiers in laser spectroscopy, proceedings of the international school of physics "Enrico Fermi": course 120*, ed. by T.W. Hänsch, and M. Inguscio (North-Holland, Amsterdam, 1994), pp. 359-376.

11. L.S. Ma, P. Jungner, J. Ye, and J.L. Hall, "Delivering the same optical frequency at two places: accurate cancellation of phase noise introduced by an optical fiber or other time-varying path," *Opt. Lett.* **19**, pp. 1777-1779, 1994.

12. H.G. Dehmelt, "Proposed $10^{14}\ \Delta\nu < \nu$ laser fluorescence spectroscopy on Tl^+ mono-ion oscillator," *Bull. Am. Phys. Soc.* **20**, p. 60, 1975.

13. J.C. Bergquist, W.M. Itano, and D.J. Wineland, "Recoilless optical absorption and Doppler sidebands of a single trapped ion," *Phys. Rev. A* **36**, pp. 428-430, 1987.

14. D.J. Wineland and W.M. Itano, "Laser cooling of atoms," *Phys. Rev. A* **20**, pp. 1521-1540, 1979.

15. R.D. Cowan, *The theory of atomic structure and spectra,* Univ. California Press, Berkeley, CA, 1981.

16. C.J. Sansonetti and J. Reader, "Spectrum and energy levels of singly-ionized mercury (HgII)," *Phys. Scripta*, (in press).

17. Th. A.M. Van Kleef and M Fred, "Zeeman effect measurements in neutral and singly ionized mercury," *Physica* **29**, pp. 389-404, 1963.

18. J.R.P. Angel and P.G.H. Sandars, "The hyperfine structure Stark effect: I. Theory," *Proc. Roy. Soc. A* **305**, pp. 125-138, 1968.

19. D.J. Berkeland, J.D. Miller, J.C. Bergquist, W.M. Itano, and D.J. Wineland, "Minimization of ion micromotion in a Paul trap," *J. Appl. Phys.* **83**, pp. 5025-5033, 1998.

20. L.S. Brown and G. Gabrielse, "Precision spectroscopy of a charged particle in an imperfect Penning trap," *Phys. Rev. A* **25,** 2423-2425, 1982**.**